

## Image quality evaluation for ICA-based compression of natural scenes

*E.M. Valero, J.L. Nieves, J. Hernández-Andrés and J. Romero*

*Departamento de Óptica, Facultad de Ciencias, Universidad de Granada*

*18071-Granada (SPAIN)*

Corresponding author: E.M. Valero (valerob@ugr.es)

### ABSTRACT

We evaluate image quality of ICA-based recovered images for six different natural images using quality indexes based on pixel-by pixel absolute and colorimetric differences. We discuss the influence of the number of basis functions used in the recovery on the evolution of quality indexes and also the compression performance capabilities with different patch sizes. The results obtained indicate that 8x8 pixels is the best choice for patch size in our collection of images. We compare compression capabilities of ICA with the JPEG algorithm, designed specifically for compression of images.

### 1. INTRODUCTION

Recently, different ICA algorithms have been applied to the efficient representation of color images and spectral functions in natural scenes<sup>1-4</sup> and have shown the advantages of ICA in comparison with Principal Component Analysis (PCA) to reduce the redundant information contained in a data set. In these studies, ICA has been applied to very different image data sets, with the resulting bases differing quantitatively but not qualitatively. Nevertheless, the influence of patch size in ICA-based image compression performance and image quality of scenes recovered using ICA bases need to be studied in more detail, especially when the illuminant is daylight, as most of the results so far have been obtained using natural scenes as input data.

Making image file sizes smaller is advantageous for transmitting files across networks and for storing libraries of images. Being able to compress a full-colour image file makes a big difference in disk space and transmission time. Extensive work has been done on image-compression algorithms, some of which have been designed specifically for human observation of compressed images. The most widely used of these is JPEG (Joint Photographic Experts Group).

ICA has recently become an important tool for modelling and understanding empirical datasets, offering an elegant and practical method for blind source separation. Most observations consist of a mixture of signals. The scientific community has paid much attention to the problem of recovering the constituent sources from the convolutive mixture, and a very convenient method for doing this is ICA. Recovery relies on the assumption that the constituent sources are mutually independent.

Finding an adequate coordinate system is an essential first step in the analysis of empirical data. Principal Component Analysis (PCA) has been used for many years to find a set of basis vectors which are determined by the dataset. The principal components are orthogonal and projections of the data onto them are linearly decorrelated. These properties can be ensured by considering only the second order statistics of the data. One of the main differences between ICA and PCA is that ICA seeks instead a transformation to coordinates in which the data are maximally statistically independent, not merely decorrelated. The assumption of most classical ICA models is that observations  $x$  are generated by a linear combination of the sources  $s$ :

$$x=As \tag{1}$$

where  $A$  is the mixing matrix of unknown elements.

Variations of these models can be found according to the probabilistic model used for describing the sources, e.g. flexible source models, which depend continuously upon their parameters, schemes that switch between two source models depending upon the moments of the recovered

sources, or else a fixed source model (single function with no explicit parameters, such as in the infomax algorithm<sup>3</sup>).

## 2. METHOD

To obtain the ICA bases, we used a set of 27 multispectral images (256x256 pixels) from Nascimento's image data set<sup>5</sup>. For each pixel, the dataset provided the spectral reflectance in the interval 410-710 nm ( $\Delta\lambda=10$  nm). We obtained the colour signals for each image by multiplying the spectral reflectance by illuminant D65. First, we performed the ICA of over 50000 patches of L,M,S cone responses. The ICA algorithm used was the Extended Infomax, which is capable of blindly separate mixed sub-Gaussian and super-Gaussian signals. Patch size was 4x4, 6x6, 8x8 and 12x12 pixels, resulting in an output of 48, 108, 192 and 432 basis functions respectively. In Figure 1, we show the basis functions obtained for the 6x6 patches ordered by energy. It shows the typical structure which has been analysed earlier<sup>3</sup>. Next, we used three of the 27-image data set (under illuminant D65) and three images of natural scenes under daylight not belonging to this dataset. Our aim was to evaluate image quality of the reconstructed images with different number of basis functions for each ICA basis and different quality indexes for a comparison between the original and reconstructed image. These indexes were standard pixel-to-pixel RMSE (averaged over the whole image,  $I_1$ ), and mean S-Cielab<sup>6</sup> colour difference ( $I_2$ ). S-Cielab takes into account both spatial and colorimetric differences between a

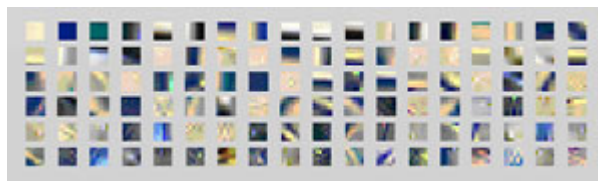


**Figure 1:** 108 ICA basis functions obtained with 6x6 patches for the 27 hyperspectral images data set. Basis functions ordered from left to right and from top to bottom.

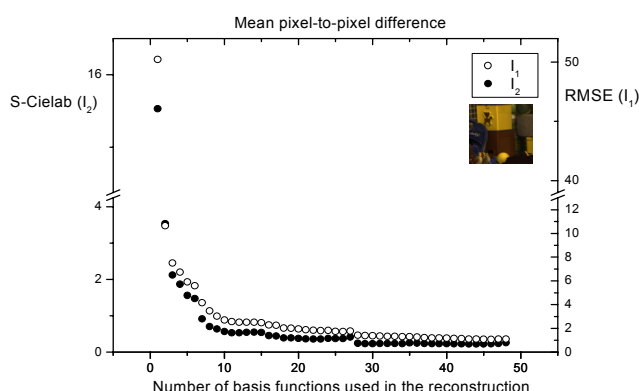


**Figure 2:**  $I_1$  and  $I_2$  for a natural scene under D65 as a function of the number of basis functions used in the reconstruction for the 4x4 patch size ICA basis.

given pair of images by performing a spatial processing in opponent-colour channels before calculating Cielab differences on a pixel-by-pixel basis.

We then estimated the number of basis functions necessary to obtain a good-quality recovered image by adopting a threshold of 10% of the maximum value of the  $I_1$  and  $I_2$  indexes. In Figure 2, we can see an example of the averaged indexes obtained for a natural scene for different number of basis functions used in the recovery with the 4x4 patch size ICA basis. The 10% of maximum difference criteria is met for 7 basis functions for both  $I_1$  and  $I_2$  indexes.

## 3. RESULTS

As we can see in Figure 2, both indexes decrease concomitantly with an increase in the number of basis functions until they become practically constant at a minimum value. For some scenes and the 4x4 patch size, the minimum value is zero for  $I_1$  and  $I_2$ , but this is not always the case. The maximum value for both indexes corresponds to recovery with only one basis function. The maximum values are quite different for  $I_1$  and  $I_2$ , and in general the 10% threshold for  $I_2$  is reached before that for  $I_1$ . For the rest of the scenes and patch sizes, the evolution of both indexes with the number of basis functions used in the recovery shows the same general trend. For the six scenes analysed, the minimum number of basis functions is 7 (4x4 patches), 6 (6x6 patches), 10 (8x8

patches) and 42 (12x12 patches) as derived from the threshold criterion. This minimum number of basis functions is not correlated to the compression limit for each scene, as the total number of basis functions for each patch size should also be taken into account.

We evaluated the compression ratio achieved by ICA as the ratio between the minimum number of data for an adequate recovery (estimated with the help of the 10% threshold criterion) and the total number of data corresponding to the uncompressed image (256x256x3 or 252x252x3 in our case). In other studies, the compression ratio is defined as the ratio between the uncompressed and compressed image (the inverse of our definition). Both are equally informative about compression capabilities. The minimum number of data for an adequate recovery depends on the minimum number of basis functions used and the number of patches in the scene. For example, for a given scene with 4x4 patch size and a minimum number of 10 basis functions, we need 10 numbers for each of the 64x64 patches of the scene ( $64=256/4$ ), and the compression ratio is given by  $(10 \times 64 \times 64) / (256 \times 256 \times 3) = 0.208$ , or 20.8%. We are aware that this compression ratio is comparing 8-bits data (uncompressed image) with 64-bits data (compressed image, as ICA coefficients are real numbers), so a saved compressed image can in principle be bigger than the uncompressed scene, but this potential drawback can be overcome if we quantize the ICA coefficients and include the maximum and minimum of the real-number distribution in the compressed file (just two 64-bits values).

In Figure 3 we show the average compression ratio for the six images used with 4x4, 6x6, 8x8 and 12x12 patch sizes. We include also an additional evaluation index which is the maximum S-Cielab difference. The compression ratio depends highly on the scene used, due to the widely different spatial and colorimetric distributions of the selected scenes, ranging from 5.2% to 41.2 % ( $I_1$  index, 8x8 patch size). So we have not included error bars in Figure 3. Compression ratios estimated by  $I_1$  are in general higher than those based on S-Cielab ( $I_2$  and maximum S-Cielab differences). From Figure 3 we can see that global compression ratio (considering the three indexes shown in the figure) is lowest (highest compression capacity) for 8x8 patch size. Thus, the results suggest that the optimal patch size for compression of this collection of scenes would be 8x8.

When the recovered image is exactly equal to the original, the indexes can reach its theoretical minimum value (zero), so the original and recovered images are virtually identical for every pixel of the scene. Nevertheless, this is not always the case. It is interesting then to study the quality of the best-achievable recovered image for each patch size. In Table 1 we show the averaged  $I_1$  and  $I_2$  for the four patch sizes used. Although there are never any visually perceptible differences between original and recovered images for 100% compression (maximum number of basis function used), we can see that as the patch size increases, the mean minimum  $I_1$  and  $I_2$  also rises. So the use of more basis functions does not necessarily improve the quality of the best recovered image. This is due to the fact that when more basis functions are added in the recovery process the last group of basis functions have very small  $L_2$ -norm and tend to be more subject to noise caused by the algorithm convergence process than the others. Thus it becomes more and more difficult to obtain a perfect recovered image as more basis functions are added in its recovery once the quality indexes have reached the flat stabilization region. When we use a patch size of 4x4 the maximum number of basis functions is 48 (4x4x3 channels), while for a 12x12 patch size is 432 (12x12x3). It is advisable then when selecting the patch size for ICA-based recovery to consider this trade-off between a worsening of the maximum quality available and compression performance.

We compared the compression ratios obtained with ICA for the optimum patch size with the most widely used compression algorithm, JPEG. When using JPEG compression, a quality index is given to the algorithm as an input, ranging generally from 0 to 100 (although this depends also on the image-treatment software used). The higher the quality index, the bigger the file size of the

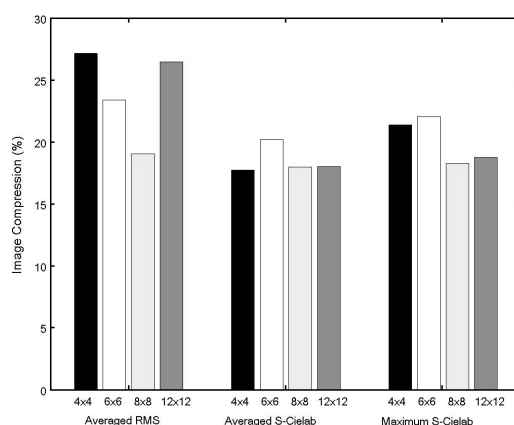


**Figure 3:** Mean compression ratios for the six images selected. Three different indexes and four patch sizes are shown.

compressed image. For the comparison we calculated the compression ratio of JPEG compressions of qualities ranging from 0 to 100 (regularly spaced 5) and the corresponding values of the  $I_1$  and  $I_2$  indexes. The compression ratio for JPEG images is calculated as the ratio between compressed and uncompressed image file size once the compressed image is saved and we have access to its file size.

**Table 1:** Average minimum  $I_1$  and  $I_2$  values for the six scenes and different patch sizes. The number of basis functions used in the recovery (maximum available) is indicated in brackets for each patch size.

Patch Size	$I_1$	$I_2$
4x4 (48)	1.83	0.55
6x6 (108)	2.04	0.59
8x8 (192)	2.04	0.60
12x12 (432)	2.07	0.65

Our results indicate that JPEG is much better than ICA in image compression performance, as the  $I_2$  index is always lower for JPEG compressed images. Mean JPEG maximum-quality compression ratio for the six scenes used are 25.3%.  $I_1$  tends to behave in the same way as  $I_2$ . The main advantage of JPEG in this case are the lower values of  $I_2$  reached for the lowest compression ratios, which indicate more similarity between original and compressed image even when there are noticeable differences between them. For some scenes ICA compression ratios are very similar to JPEG (maximum quality) capabilities, although quality indexes are always lower for JPEG compressed images with a given compression ratio. This is not very unexpected as compression is not the main purpose guiding the design of the ICA algorithm.

#### 4. CONCLUSIONS

We have used two quality-evaluation indexes that allow us to estimate computationally the compression performances for different algorithms of image compression, including ICA, which is not obviously designed for this purpose. The threshold criterion of 10% maximum index allows us to estimate both the number of minimum basis functions for optimum recovery and the compression ratio achievable by ICA. Both parameters are highly dependent on the spatial and colorimetric distribution of the image, so we have selected six very different scenes and looked for the general trends present when analysing the results. We have shown that the best performance corresponds to 8x8 patches for our set of natural scenes, and also that for the lowest compression ratios (small image file sizes) JPEG compressed images are more similar to the original than ICA-based compressed images. .

#### References

1. P.O. Hoyer and A. Hyvärinen, "Independent Component Analysis Applied to Feature Extraction from Colour and Stereo Images," *Network: Computation in neural systems* 11, 191-210 (2000).
2. D.R. Taylor, L.H. Finkel and G. Buchsbaum, "Color Opponent Receptive Fields Derived from Independent Component Analysis of Natural Images," *Vision Research*, 40, 2671-2676 (2000).
3. T. Wachtler, T.-W. Lee, and T.J. Sejnowski, "Chromatic structure of natural scenes," *J. Opt. Soc. Am. A* 18, 65-77 (2001).
4. T.-W. Lee, T. Wachtler, and T.J. Sejnowski, "Color Opponency Constitutes A Sparse Representation For the Chromatic Structure of Natural Scenes," *Vision Research*, 42, 2095-2103 (2002).
5. S. M. C. Nascimento, F.P. Ferreira, and D.H. Foster, "Statistics of spatial cone-excitation ratios in natural scenes," *J. Opt. Soc. Am. A* 19, 1484-1490 (2002).
6. X. Zhang and B.A. Wandell. "A spatial extension of Cielab for digital color image reproduction," *SID Digest* 19, 27-31 (1996).